NASA Technical Memorandum 102021

Test Facility and Preliminary Performance of a 100 kW Class MPD Thruster

(NASA-TM-102021) TEST FACILITY AND PRELIMINARY PERFORMANCE OF A 100 kW CLASS MPD THRUSTER (NASA. Lewis Research Center) 21 p
CSCL 21C
N89-23520
Unclas
G3/20 0210304

James S. Sovey, Maris A. Mantenieks,
Thomas W. Haag, and Paul Raitano
National Aeronautics and Space Administration
Lewis Research Center
Cleveland, Ohio

and

James E. Parkes
Sverdrup Technology, Inc.
NASA Lewis Research Center Group
Cleveland, Ohio

Prepared for the
1989 JANNAF Propulsion Meeting
Cleveland, Ohio, May 23–25, 1989

NASA

TEST FACILITY AND PRELIMINARY PERFORMANCE OF A 100 kW CLASS MPD THRUSTER

J. S. Sovey, M. A. Mantenieks,
T. M. Haag, and P. Raitano
National Aeronautics and Space Administration
Lewis Research Center
Cleveland, Ohio

and

J. E. Parkes
Sverdrup Technology, Inc.
NASA Lewis Research Center Group
Cleveland, Ohio

E-4742

ABSTRACT

A 260 kW magnetoplasmadynamic thruster test facility was assembled and used to characterize thrusters at power levels up to 130 kW using argon and helium propellants. Sensitivities of discharge characteristics to arc current, mass flow rate, and applied magnetic field were investigated. A thermal efficiency correlation developed by others for low power MPD thrusters defined parametric guidelines to minimize electrode losses in MPD thrusters. Argon and helium results suggest that a parameter defined as the product of arc voltage and the square root of the mass flow rate must exceed 0.7 V-kg$^{1/2}$-sec$^{-1/2}$ in order to obtain thermal efficiencies in excess of 60 percent.

INTRODUCTION

The magnetoplasmadynamic (MPD) thruster has propulsion applications for Earth-orbit transfer, maneuvering of large space systems, and interplanetary missions. The high thruster specific impulse (1000 to 5000 sec) minimizes propellant requirements and the demands for mass transfer to low-Earth-orbit. Potential MPD thruster missions in the next few decades will probably employ solar or nuclear electric power systems in the 30 to 300 kW range. Farther term missions with interplanetary propulsion applications could use megawatt class nuclear power systems.

Over the last three decades, a significant effort has been expended in characterizing the performance and life of pulsed and steady-state MPD thrusters.[1-3] Most researchers have used pulsed or quasi-steady state MPD thrusters because of thruster/power system simplicity and modest vacuum facility requirements. Pulsed thrusters, operating for about 1 msec, are the only source of data concerning the discharge phenomena and performance limits of 1 to 10 MW class MPD arcjets.

The most attractive specific impulse and thrust efficiency data to date result from thrusters using hydrogen or lithium propellants.[3] Since lithium propellant may not be desirable because of potential spacecraft and ground test facility contamination issues, it is likely that steady-state thruster applications will involve the use of hydrogen or hydrogenic propellants. The power, thermal, and vacuum system requirements for megawatt class steady-state thrusters operating with hydrogenic propellants exclude the use of most of the existing vacuum facilities in the United States. For example, a vacuum environment of less than 4×10^{-2} Pa (3×10^{-4} torr) is generally required to minimize the background gas entrainment effects on thruster performance.[4] Prior to 1972, a large percentage of the data for 10 to 100 kW inert gas, ammonia or hydrogen thrusters was obtained at vacuum facility pressures in excess of 1.3 Pa (1.0×10^{-2} torr). It was shown that thrust uncertainties of 50 to 100 percent could exist because of gas entrainment in applied field devices.[3,4] More recently, self-field, steady state MPD thrusters using argon and nitrogen have been evaluated at vacuum tank pressures between 1 and 2.7 Pa.[5] These results showed that, for powers up to 75 kW, reliable self-field thruster data could be obtained at facility pressures less than 1.3 Pa.

This paper describes a new MPD thruster test facility capable of providing reliable performance data for steady-state, self and applied-field MPD thrusters operating in the 20 to 250 kW power range. The test facility includes the vacuum chamber, power supplies, water cooling system, propellant metering, and thrust stand. Preliminary performance of a series of thrusters operated at arc currents from 500 to 3000 A using a variety of inert gases is described. Basic performance parameters discussed are discharge characteristics, starting transients, magnetic field effects and thermal efficiencies.

THRUSTER AND MAGNET ASSEMBLY

The MPD thruster used in this investigation was derived from a commercial coaxial plasma generator that is commonly used for plasma spraying.[6] This commercial device was selected because it was capable of routinely operating at 30 to 60 kW for extended periods of time and could be used

immediately to checkout the new test facility. The device, shown in Fig. 1, was comprised of a copper anode assembly in which the water circuit was connected in series with the cathode water cooling hardware. Anode channel diameters are listed in Table I. The anode channel extended from the upstream end of the thoriated tungsten cathode to the thruster exit plane. The 13 mm diameter, 2 percent thoriated tungsten cathode was brazed to a water-cooled copper retainer. Cathode length was defined as the length of the exposed tungsten cathode. Water flow rates ranged from 0.4 to 0.7 liter/sec depending on the anode design. The thruster assembly was usually sealed with O-rings. O-rings near the cathode base were sometimes replaced with metal gaskets to minimize the risk of O-ring decomposition at high arc currents. The anode and cathode were isolated using fluropolymer and alumina insulators. The basic plasma generator could be easily retrofitted with different anode and cathode designs. For example, a flared anode design is shown in Fig. 2.

Plasma sprayers operate as thermal arcs with inlet pressures usually greater than 1 atm. In order to enhance the electromagnetic thrust component the anodes were designed with larger channels, the current range was extended to 3000 A, the mass flow rates were reduced to provide inlet pressures between 1.3 and 13 kPa (10 to 100 torr), and magnetic fields as high as 0.3 T were applied. These changes enhanced the electromagnetic acceleration of the plasma. Values of $J^2/\dot{m}$ ranged from $1x10^{10}$ to $3x10^{11}$ A^2-sec/kg, values which generally imply a significant electromagnetic thrust contribution.[3,7] Increases in the $J^2/\dot{m}$ parameter resulted in higher specific impulse operation and ultimately led to the onset of discharge instabilities.[8]

For all tests, the anode channel to cathode radius ratios were restricted to less than 2.05 because of water cooling requirements. Radius ratios in the 3 to 5 range have been found to significantly enhance thrust, implying that anode geometries with small channels probably will not lead to highly optimized performance.[9,10] The thruster served as a rugged test article for evaluation of the test-stand and also provided baseline MPD thruster data in the 10 to 80 kW range at low vacuum facility pressures. Table I shows the dimensions of the four thruster configurations that were evaluated. Parametric variations involved anode diameter, anode channel length, and the degree of anode flare.

A solenoid applied-magnetic field was used with the MPD thruster because previous experiments indicated this could enhance performance and improve anode life by preventing arc attachment on the anode in the form of localized spots.[2,11,12] The magnet was designed to provide a magnetic field of a few tenths of a Tesla at the center of the magnet for a magnet current of 1500 A. Relatively high specific impulse measurements have been obtained from low power MPD thrusters using 0.1 to 0.2 T magnetic fields.[3] Calculations showed that 0.2 T fields could be obtained by using about 46 turns on a 14 cm diameter spool.[13] Copper tubing, with a 1.3 cm outside diameter and a 0.89 mm wall, was selected to minimize coil resistance and to provide adequate water flow rates for magnet cooling. Glass sheath insulation was used to prevent tube-to-tube shorting. The magnet, shown in Figs. 3(a) and (b), had four layers of ten coils each, and a final layer with six coils. The number of coils in the final layer was chosen primarily for ease of assembly. The electromagnet envelope was approximately 15 cm long with a 28 cm outside diameter and a 14 cm inside diameter. The magnet tubing provided a passage for about 0.3 liter/sec of water cooling. Maximum available coil current was 1500 A.

Measured and calculated axial magnetic field strengths are compared in Fig. 4. The locations of cathode and anode exit plane are shown as bands in Fig. 4 since the relative location of the thruster and magnet was sometimes changed during the course of testing. The field strength was calculated using equations developed in Ref. 13. The axial field strengths measured in the region of the cathode tip and the thruster exit plane were about 0.23 and 0.16 T, respectively, for a magnet current of 1400 A. The magnet coil wall thickness of 0.89 mm resulted in a power dissipation of about 49 kW at 1400 A. Magnet power was not considered in any of the thruster efficiency analyses.

TEST FACILITY

The test facility consisted of the vacuum chamber, a propellant metering panel, water-cooling apparatus, the thrust stand, the power system, and a data acquisition system. This section provides detailed descriptions of each of these systems, the procedures used, and the results of calibration and diagnostic measurements.

VACUUM CHAMBER

The thruster and thrust stand were mounted to a vacuum chamber bulkhead and were inserted into a 3 m diameter by 3 m long port as shown in Fig. 5. The port (or spoolpiece) could be separated from the 7.6 m diameter by 21 m long main vacuum chamber by a gate valve. The vacuum chamber was evacuated using nineteen 0.8 m diameter hydrocarbon oil diffusion pumps with freon traps cooled to 236 K. The no-flow main chamber pressure was approximately $2.0x10^{-4}$ Pa ($1.5x10^{-6}$ torr). Pressures during normal MPD thruster operation were maintained below $8x10^{-2}$ Pa to prevent collapse of the oil diffusion pumps and to minimize heating of the intermediate stage rotary pumps. For example, a nitrogen flow rate of $1.0x10^{-4}$ kg/sec would produce a pressure of $8x10^{-2}$ Pa in the main chamber. Facility pressures were monitored in the 3 m port and in the main chamber at locations of 12 and

16 m downstream of the thruster. The pressures for hydrogen, helium, neon, and argon were obtained by multiplying the indicated readings by gas correction factors of 2.4, 5.6, 3.2, and 0.70, respectively.[14]

Figure 6 shows the vacuum chamber pressure-mass flow rate calibration for argon, helium, and neon. The calibration was undertaken by using cold-gas flow. The pressure was sensed in the main chamber approximately 12 m from the thruster. Thruster data were taken with either 15 or 19 diffusion pumps operational. Maximum flow rates for helium, nitrogen, and argon were about 4.5, 8.0, and 15×10^{-6} kg/sec, respectively, when the main chamber pressure was 7×10^{-2} Pa (5×10^{-4} torr). It is estimated that the MPD thruster could be operated at power levels in excess of 200 kW in the test facility and still maintain satisfactory diffusion pump operation. Such an estimate is based on a $J^2/\dot{m}$ of 1×10^{11} A^2-sec/kg, an argon flow rate of 1.5×10^{-4} kg/sec, and an arc voltage of about 50 V.

During the initial operational tests of the facility, an arcjet was operated from 20 to 130 kW with argon and helium for periods of 1 to 3 hr. In Fig. 7, atomic excitation in the plume of the 130 kW helium arcjet is shown to extend at least 4 m downstream of the thruster. In this case, the high helium flow rates precluded use of the diffusion pumps, so only the rotary blowers and roughing-pumps were operating. The thermal load from the arcjet exhaust was spread over a large area of the 7.6 m diameter by 21 m chamber. A 0.9 by 1.4 m molybdenum sheet metal panel was placed about 15 m from the thruster to intersect some of the exhaust. During tests with a duration of a few hours, the vacuum facility surfaces never reached temperatures that would be a cause for concern for O-ring or viewing port failure. Short term tests of a few hours were adequate for performance characterization, plasma diagnostics, and some electrode erosion diagnostics.

PROPELLANT FEED SYSTEM

The propellant feed system was designed to provide three parallel gas paths such that one or more gases might be available for thruster operation. The selected gas passes to an accumulator from the multiple gas panel. Accumulator pressures were approximately 0.2 MPa. One of three sensors could then be selected to monitor the flow rate. Ranges were 0.5, 5, and 50 standard liters of nitrogen per minute. Precision flow control valves were located downstream of the flow meters. Flowmeter accuracy was estimated to be less than 2 percent over the range of 10 to 100 percent of full-scale. Flowmeters were directly calibrated with argon and helium. Estimates of nitrogen and neon flow rates were based on the vendor's calibration factors.

Thruster inlet pressure was sensed using a capacitance manometer. Inlet pressures were generally in the 4 to 16 kPa range. While the thruster chamber pressure was not directly measured due to the significant pressure drop across the thruster propellant injector, the inlet pressure provided an upperbound of the thruster chamber pressure.

COOLING AND CALORIMETER SYSTEM

Water cooling to the arc and magnet was provided by two separate pump/heat exchanger assemblies capable of supplying 0.8 liter/sec of water at a pressure of 1 MPa. De-ionized, distilled water provided cooling in a closed-loop system. The heat exchanger was cooled using the laboratory water system. The closed-loop water flowed through polymer hose to feed-throughs in the vacuum bulkhead and on to the power and water junction located about 1.5 m inside the 3 m port. Water then flowed to the thruster through the power cables. Two other closed-loop refrigeration systems were available to pump 0.03 liter/sec of water to diagnostic probes or cathode assemblies.

The MPD thruster cathode and anode were cooled by the same pump/heat exchanger. Water flow rate data were obtained from a calibrated turbine meter. The power lost to the electrodes was obtained by measuring the water flow rate and the change in water temperature.

THRUST STAND

The thrust stand must provide a high resolution measurement of low thrust given the fact that the thrust to weight ratio of an MPD device is less than 0.01. Thrust tares due to electromagnetic fields, vibration, and thermal drift were of major importance. The thrust stand, shown in Fig. 8, is an inverted pendulum whose upright flexures deflect about 5 cm at a thrust of 5 N. The pivoting structure of the thrust stand transferred the weight of the thruster to a system of flexures anchored to the lower frame. The primary flexures consisted of two 16 mm diameter copper tubes which were 60 cm long. The flexures pivoted about an axis 1.5 m below the thruster centerline as shown in Fig. 8. The 16 mm copper tubes carried the MPD arcjet current and cooling water. Current to the magnet terminals was supplied by two pairs of 9 mm diameter copper tubes. Gas was fed through a single 6 mm diameter tube, and 22 flexible linkages transferred the instrumentation signals. The major restoring force was provided by the 16 mm diameter primary flexures. The time derivative of the thrust stand displacement was used to drive an electromagnetic damper. The damper was active only during brief perturbations and did not affect steady state thrust measurement.

Thrust stand displacement was measured by a movable iron core in a linear variable differential transformer (LVDT) which was mounted to a fixed reference structure. The thrust stand assembly contained a remotely controlled leveling mechanism to vary the angle of the stand and adjust the LVDT signal. The remote thrust stand leveling was required since the inclination of the stand would change after the vacuum chamber was evacuated. Remote calibration of the stand was obtained by applying small weights along the thrust axis using monofilament line and a precision pulley. The weights applied a force in the thrust direction, and the subsequent deflection was sensed by the LVDT (Fig. 8). In addition to applying the calibration weights, a small motor activated a lock-up lever so the thrust stand could be safely inserted into and retracted from the vacuum chamber.

The thrust stand was evaluated using the water-cooled MPD thruster. The thrust stand displacement signal showed no evidence of thermal drift. The thrust measurement uncertainty due to thermal drift and vacuum facility induced vibration was measured to be less than 5×10^{-3} N. This uncertainty is very small since a 50 kW thruster with an overall efficiency of 30 percent at a specific impulse of 3000 sec will produce a thrust of about 1 N. However, thrust stand displacement errors due to magnetic interactions have not yet been resolved. Thruster arc currents of 3000 A and applied field strengths of about 0.3 T have resulted in errors as high as 0.5 N. Design modifications to minimize the electromagnetic tares are in progress.

POWER SYSTEM

The power system was primarily composed of the arc supply, a high voltage arc starter, the magnet supply, and safety sensors and interlocks. The arc supply consisted of four welding power supplies connected in a series-parallel arrangement as shown in Fig. 9. The welding supplies were controlled by magnetic amplifiers; typical features are described in Ref. 15. The arc supply was isolated from vacuum facility ground to minimize extraneous arcing. Line power to the arc supply was 460 V, 3 phase and 60 Hz. Maximum output power capability was 264 kW at 3000 A and 88 V. Figure 10 shows the general layout of the four arc power supplies, the magnet supply, power cables, and water-cooled diodes. The open circuit voltage was 160 V. Arc current was monitored using a 3000 A, 50 mV shunt. During normal arc operation and resistive load-bank tests, the peak-to-peak voltage ripple was about 5 percent of the dc level over a 1000 to 2000 A current range. Current ripple could not be obtained because of electromagnetic interference to the low voltage shunt signal which was sensed by an electrically floating oscilloscope. Two 2000 A shunts were used to check the current balance in the series-parallel arrangement. Currents from power supplies (1, 2) and (3, 4) were usually balanced to within 5 percent (Fig. 9). Arc voltage was obtained from potential leads at the MPD thruster. The arc-starter power supply was a half-wave rectifier connected to the MPD thruster through a 100 Ω current limiting resistor. The starter supply provided an open circuit voltage of 950 V and a steady-state current of about 0.6 A.

The power cables consisted of four-28 mm diameter copper cables sized conservatively to handle 750 A each. Each cable contained 1925 strands of 0.056 cm diameter wire. A total of eight water-cooled, 25 mm diameter copper rods served as the vacuum feed-throughs for thruster power. Feed-through water-cooling was provided by the laboratory water system. The cables extended about 1.5 m into the 3 m diameter port to a water-cooled junction. This water and power junction provided flexibility in routing the water lines and power cables directly to thrusters or to the thrust stand. Two pairs of water-cooled stranded copper cables were connected from the power junctions to the arc electrodes or the thrust stand power terminals. On some occasions, each pair of water-cooled stranded copper cables was replaced by a 16 mm diameter, 1.2 mm wall copper tube which carried the arc current and cooling water. All exposed metal conductors were wrapped with silicone tape to prevent arcing to the power cables.

Figure 9 also shows a 5500 A, water-cooled diode which provided high voltage protection for the arc supply. A metal oxide varistor was incorporated to provide a current path if voltage transients, upstream of the high current diode, exceeded 175 V.

The arc was started by setting the argon flow rate to approximately 4.4×10^{-4} kg/sec, initiating a low current glow discharge from the starter supply, and activating the arc supply which was preset for 2000 A operation. Four seconds after arc ignition, the arc current was reset to 1000 A, the arc starter was turned off, and the flow rate was reduced to about 9.0×10^{-5} kg/sec which was more typical of the low pressure MPD arc. As indicated in Fig. 11, the arc current rose to about 5000 A in 7 ms and was near the preset current level at 0.5 sec. This procedure heated the cathode rapidly and usually showed very little evidence of ejected electrode material. In all cases, the arc was started with argon. Transition to another propellant was accomplished by closing the argon isolation valve and opening the valve for the desired propellant. This transition took about 10 min due to the large accumulator volume. The arc could also be started by setting the argon flow rate at 9.0×10^{-5} kg/sec, establishing the arc supply open circuit voltage, turning on the starter supply, and finally providing a short duration (<1 sec), high pressure argon pulse. A brief high pressure gas starting pulse was desired to prevent overloading the vacuum facility with propellant and causing collapse of the diffusion pump jets and heating of the rotary pumps. An automated sequencer starting process is now under development.

During arcjet operation, the anode potential was found to float within 10 V of facility ground at argon flow rates in excess of 4.0×10^{-5} kg/sec. However, the anode floated to about 40 V above ground at very low flow rates of 8.0×10^{-6} kg/sec. In all cases there was very little evidence of arcing external to the thruster as long as the arc supply was floating, power cables were insulated, and the facility pressure was less than 7×10^{-2} Pa.

A single welding supply provided power to the electromagnet. Maximum steady state current was 1500 A. The peak-to-peak, current ripple was about 20 percent of the dc level for magnet currents from 1000 to 1400 A. The power supply was isolated from ground as well as from the arc supply. A blocking diode was inserted in the circuit in the event that the magnet was referenced to anode potential. A diode was placed in parallel with the supply to soften any turn-off transients that might be caused by the high inductance load.

The MPD thruster system was interlocked for safety purposes as well as to protect the vacuum chamber and the thruster. Table II details the system sensors and actions taken in the event of abnormal operation.

PRELIMINARY THRUSTER PERFORMANCE

Preliminary experiments with the MPD thruster were directed at determining the discharge characteristics and the sensitivity of the discharge parameters to geometry, flow rate, and applied magnetic field. Nearly all of the performance characteristics were obtained at inlet pressures between 4 and 16 kPa (30 to 120 torr). Finally, insight into thruster performance was obtained by documenting the thruster thermal efficiency over a wide range of parameters. Thrust tares due to magnetic forces precluded reporting overall thruster performance.

DISCHARGE CHARACTERISTICS

Figure 12 displays arc voltage versus arc current for small and large anode channel thrusters. Electromagnet currents in the 0.8 to 1.4 kA range were used, resulting in magnetic fields at the cathode tip from 0.14 to 0.23 T. The argon thrusters with straight cylindrical channels generally exhibited V-J characteristics with a negative slope at arc currents less than 1500 A. Such characteristics are typical of high pressure thermal arcs[16] rather than low pressure MPD arcs which generally have positive V-J characteristics.[17] Thruster B, with the 16.5 mm channel, generally operated with arc voltages less than 25 V. When the larger channel thruster (C) was operated at arc currents between 1 and 2 kA, the arc voltage was in the 25 to 40 V range depending upon the selected values of flow rate and applied magnetic field. In order to preserve discharge stability, the magnetic field at the cathode had to be at least 0.04 T for all four thruster geometries tested (Table I). Figure 12 also shows that, at a magnet coil current of 800 A, the arc exhibited a dual voltage mode characteristic which has been observed by many investigators.[18] Instabilities and dual mode operation were minimized or did not exist at the high magnetic fields and arc currents in excess of 1500 A. As indicated in Ref. 18, the low voltage mode was thought to be caused by arc attachment near the upstream end of the anode channel while the high voltage mode is caused by a major portion of the arc current attaching near the channel exit plane. It was also speculated that as the ratio of "downstream current" to total arc current is increased, a positive V-J characteristic results and the thrust and thrust efficiency increase significantly.

Thruster characteristics were documented at conditions representative of high specific impulse operation where electromagnetic forces are likely to dominate the electrothermal thrust component. The figure of merit was the $J^2/\dot{m}$ parameter which has been used as an indicator of acceleration mechanisms.[7] For example diagnostic measurements have indicated that an argon MPD thruster operated at a $J^2/\dot{m}$ of 3.8×10^{10} A^2-sec/kg had an electromagnetic thrust component of about 98 percent; this component was reduced to 50 percent with a $J^2/\dot{m}$ of 3.4×10^9 A^2-sec/kg.[19]

The small channel diameter MPD thruster may not be of much interest because of its low arc voltage and high electrode losses, but it was capable of operating stably at values of $J^2/\dot{m}$ in the 1.4×10^{11} to 3.5×10^{11} A^2-sec/kg range. These devices may be of value in studying discharge stability criteria and limits.

Figure 13 shows the V-J characteristics for helium and neon using the small channel thruster. The arc voltage of helium was about twice the argon value using Thruster B. The helium V-J characteristics indicated higher arc voltages were obtained with a shorter anode channel even at twice the mass flow rate. More detailed studies of discharge characteristics are required to better understand these phenomena. The sensitivity of arc voltage to argon mass flow rate is shown in Fig. 14. The data at 4.5×10^{-4} kg/sec are representative of a thermal arc operating with an inlet pressure of nearly one atmosphere. All other data points have $J^2/\dot{m}$ parameters greater than 2×10^{10} A^2-sec/kg and are thought to represent conditions where electromagnetic forces dominate the thrust.[19]

Since the anode losses generally increase monotonically with arc current, the power available to the plasma may be optimized at higher arc voltages so losses associated with the anode drop,

electron heating, and electron absorption at the anode are relatively small.[20] Figure 14 indicates the MPD arc voltage was nearly doubled by increasing the anode channel area by a factor of 2.5. This conclusion is not compromised by the fact that the arc currents are not identical since the arc voltage of Thruster B is rather insensitive to arc current in the 1 to 2 kA range. The impact of these results on thermal efficiency will be discussed in the next section.

The sensitivity of arc voltage to applied magnetic field using the large channel thruster is shown in Fig. 15. Dual voltage mode argon operation was exhibited with Thruster C at an arc current of 1500 A and magnet currents below 800 A. The dual voltage mode did not exist at an arc current of 2000 A. The discharge voltage was increased by about 80 percent as the magnet current was varied from 500 to 1400 A. These magnet currents corresponded to magnetic fields of 0.075 to 0.23 T in the vicinity of the cathode. The flared anode exhibited higher arc voltages than the straight channel thruster. It is hypothesized that the anode flare promoted "downstream arc attachment" and higher arc voltages.

THERMAL EFFICIENCY

A large fraction of the MPD thruster input power was deposited in the electrodes at input power levels up to about 300 kW. For example, in previous work the maximum power available for thrust production with hydrogen, ammonia, and argon MPD arcjets was found to be typically 80, 70, and 60 percent of the input power, respectively.[5,12,21] These data were obtained from water-cooled devices which are less efficient and are presumed to have larger anode voltage drops than radiation cooled MPD thrusters.[2]

Figure 16 compares the thermal efficiency of Thrusters B and D with specific power as the independent variable. Specific power is simply defined as the ratio of electric power to mass flow rate. The thermal efficiency is:

$$\eta_{th} = \frac{P_e + P_o - P_R}{P_e + P_o} \approx 1 - \frac{P_R}{P_e} \qquad (1)$$

The cold gas power, P_o, was neglected in the calculations since it was less than 0.3 percent of the electric power for all data reported. At specific powers greater than 3.7×10^8 J/kg about 90 percent of the input power was deposited in the electrodes of the small channel thruster (B). The large channel thruster (D) with the flared anode had thermal efficiencies of 30 to 53 percent. Since Thruster D exhibited arc voltages that were generally 15 to 20 V higher than voltages of the small channel thruster (B) at arc currents of 1500 to 2000 A, the ratio of anode fall to arc voltage was probably smaller using the large channel thruster (D).

Thermal efficiencies for the large channel thruster (D) decreased with increasing specific power. This result was not unexpected since the arc voltage generally decreased or remained relatively constant with increasing arc current, so that the fractional energy losses associated with the anode fall voltage, electron heating, and work function became relatively large. An effective anode fall voltage defined as:

$$V_e = \frac{P_R}{J} \qquad (2)$$

has been used by others in describing anode loss phenomena.[1] In Fig. 17, the effective anode fall voltage is plotted against specific power for argon, helium, and neon propellants. Thermal arcs, operating at specific powers of 37 to 125 MJ/kg, had an effective anode fall voltage of 10 to 15 V. The MPD thrusters operating at higher specific powers and inferred higher specific impulse had effective anode fall voltages of 20 to 30 V which were a major fraction of the arc voltage measured using Thrusters A to D.

MPD thruster experiments by Cann, et al.[20] indicated that the anode power losses varied linearly with arc current at fixed flow rate. The anode loss was also found to vary as the reciprocal square root of the mass flow rate at fixed arc currents. These relationships were indicative of the convection of electron energy with the arc current, and such effects had been found to exist in arcjets dominated by Joule heating.[22] Assuming

$$P_R = GJ\dot{m}^{-1/2} \qquad (3)$$

where the parameter G depends on the type of propellant[22] then

$$\eta_{th} = 1 - \frac{G}{\dot{m}^{1/2}V} \qquad (4)$$

These simple relationships prompted the selection of $\dot{m}^{1/2}V$ as the correlating parameter for the thermal efficiency data for argon, helium, nitrogen and neon. A clear parametric relationship

between the thermal efficiency data and arc current, $J^2/\dot{m}$, power, or specific power was not evident. The data shown in Fig. 18 were taken between 1 and 3 kA. The thermal efficiency is very sensitive to the $\dot{m}^{1/2}V$ parameter in the 0.13 to 0.32 V-kg$^{1/2}$-sec$^{-1/2}$ range. Although the results for all gases did not follow the simple relation of Eq. (4), the thermal efficiency increased monotonically with $\dot{m}^{1/2}V$ up to about 0.5 V-kg$^{1/2}$-sec$^{-1/2}$. The data where the thermal efficiency appears to approach an asymptote are thermal arc results (high flow rates and dominant Joule heating). A least-squares, fourth order polynomial fit for thermal efficiency versus log ($\dot{m}^{1/2}V$) had a correlation coefficient of 0.87. This correlation is good considering the data of Fig. 18 were obtained using four propellants, four thruster geometries, currents from 1 to 3 kA, and mass flow rates from 8×10^{-6} to 4.5×10^{-4} kg/sec.

The correlation curve in Fig. 18 can also be compared to data obtained by others with ammonia and argon. Figure 19 shows 100 kW class argon thruster results from the University of Stuttgart[5] and ammonia data taken at NASA Lewis Research Center in 1970.[23] These results were consistent with the η_{th} - ($\dot{m}^{1/2}V$) curve developed in Fig. 18. These ammonia and argon data are within ±17 percent of the thermal efficiency curve. For comparison purposes, thermal efficiency estimates from a pulsed megawatt thruster are also shown in Fig. 19.[24] All data suggest that the MPD thrusters be operated at values of $\dot{m}^{1/2}V$ greater than 0.7 V-kg$^{1/2}$-sec$^{-1/2}$ in order to minimize electrode losses. At the same time, the $J^2/\dot{m}$ parameter must be driven to sufficiently high levels to ensure relatively large electromagnetic acceleration and high specific impulse levels in the 2000 to 5000 sec range.

CONCLUDING REMARKS

A steady-state MPD thruster test facility was assembled, including a 260 kW power system, electrode cooling apparatus, thrust stand, feed system, data system and a vacuum chamber capable of pumping 1.0×10^{-4} kg/sec of nitrogen at about 0.08 Pa. The operational capability of the test facility was characterized using MPD and thermal arcjets at power levels up to 80 and 130 kW, respectively. The thrust measurement uncertainty due to thermal and vibration effects was less than 5×10^{-3} N which is about 0.5 percent of the thrust produced by a 50 kW argon thruster. However, modifications are required to minimize thrust stand displacements due to magnetic forces caused by power cables and the electromagnet.

The sensitivities of discharge characteristics to arc current, mass flow rate, and applied magnetic field were investigated using four thruster geometries. All MPD thrusters had anode channel diameters of 26 mm or less and generally exhibited negative V-J characteristics which are thought to be caused by the majority of the arc current attaching near the upstream end of the anode channel.

Higher arc voltages and thermal efficiencies were obtained using the larger anode channel (26 mm) device with a flared anode. Representative anode fall voltage, estimated by anode losses, were in the 15 to 30 V range for the argon and helium MPD arcjets. All thermal efficiency results correlated well with the product $\dot{m}^{1/2}V$ parameter. Argon and helium data suggest that $\dot{m}^{1/2}V$ must be greater than 0.7 V-kg$^{1/2}$-sec$^{-1/2}$ to obtain thermal efficiencies in excess of 60 percent. At the same time, the $J^2/\dot{m}$ parameter must be sufficiently high to provide specific impulse values of interest.

NOMENCLATURE

G	parameter that depends on type of propellant, V-kg$^{1/2}$-sec$^{-1/2}$
J	arc current, A
J_m	magnet current, A
$\dot{m}$	mass flow rate, kg/sec
P_e	electric power, W
P_l	power loss to the electrodes, W
P_o	inlet cold gas power, W
$P_e/\dot{m}$	specific power, J/kg
V	arc voltage, V
V_e	effective anode fall voltage, V
η_{th}	thermal efficiency

ACKNOWLEDGMENTS

The authors wish to acknowledge the assistance of Michael R. LaPointe and Roger M. Myers in the magnetic field analyses and arc transient measurements, respectively. The technical support in the assembly of the MPD thruster test facility by David R. Hoffman, Charles A. Rueger, Gerald F. Schneider, James H. Potantus, Robert D. Buttler, David R. Lilly and Stephen M. Cuglewski is deeply appreciated.

REFERENCES

1. Nerheim, N.M.; and Kelly, A.J.: A Critical Review of the State-of-the-Art of the MPD Thrustor. AIAA Paper 67-688, Sept. 1967.

2. Seikel, G.R.; York, T.M.; and Condit, W.C.: Applied-Field Magnetoplasmadynamic Thrusters for Orbit-Raising Missions. Orbit-Raising and Maneuvering Propulsion: Research Status and Needs, (Progress in Astronautics and Aeronautics, Vol. 89), L. H. Caveny, Ed., AIAA, 1984, pp. 260-286.

3. Sovey, J.S.; and Mantenieks, M.A.: Performance and Lifetime Assessment of MPD Arc Thruster Technology, AIAA Paper 88-3211, July 1988. (NASA TM-101293).

4. Sovie, R.J.; and Connolly, D.J.: Effect of Background Pressure on Magnetoplasmadynamic Thruster Operation. J. Spacecraft Rockets, vol. 7, no. 3, Mar. 1970, pp. 255-258.

5. Kurtz, H.L.; Auweter-Kurtz, M.; and Schrade, H.O.: Self-Field MPD Thruster Design - Experimental and Theoretical Investigations. AIAA Paper 85-2002, Sept. 1985.

6. Product Data Sheet 387-1, Electro-Plasma, Inc., Irvine, CA, 1988.

7. Halliaris, A.C.; John, R.R.; Garrison, R.L.; and Libby, D.R.: Quasi-Steady MPD Propulsion at High Power. (AVSD-0146-71-RR, Avco Corp.; NASA Contract NAS1-9939) NASA CR-111872, 1971.

8. Barnett, J.W.; and Jahn, R.G.: Onset Phenomena in MPD Thrusters. AIAA Paper 85-2038, Oct. 1985.

9. Jahn, R.G.: Physics of Electric Propulsion, McGraw Hill, Inc., 1968.

10. Wolff, M.; Kelly, A.J.; and Jahn, R.G.: A High Performance Magnetoplasmadynamic Thruster. 17th International Electric Propulsion Conference, Japan Society for Aeronautical and Space Sciences, Tokyo, Japan, 1984, pp. 206-212.

11. Ducati, A.C.; Huehlberger, E.; and Todd, J.P.: Design and Development of a Thermo-Ionic Electric Thruster. NASA CR-59804, 1964.

12. Ducati, A.D.; Huehlberger, E.; and Giannini, G.: High Specific Impulse Thermo-Ionic Acceleration. AIAA Paper 64-668, Aug. 1964.

13. Brown, G.V.; Flax, L.; Itean, E.C.; and Laurence, J.C.: Axial and Radial Magnetic Fields of Thick, Finite-Length Solenoids. NASA TR-R-170, 1963.

14. Holanda, R.: Sensitivity of Hot-Cathode Ionization Vacuum Gages in Several Gases. NASA TN-D-6815, 1972.

15. Kloeffler, R.G.; Horrell, M.N.; and Hargrave, L.E. Jr.: Basic Electronics, Second Edition, John Wiley and Sons Inc., 1963.

16. Kuninaka, H.; Ishii, M.; and Kuriki, K.: Experimental Study on a Low-Power Direct Current Arcjet. J. Propulsion Power, vol. 2, no. 5, Sept.-Oct. 1986, pp. 408-413.

17. Tahara, H.; Yasui, H.; Kagaya, Y.; and Yoshikawa, T.: Development of a Quasi-Steady MPD Arcjet Thruster for Near-Earth Missions. AIAA Paper 87-1001, May 1987.

18. Sasoh, A.; Solem, A.E.; and Arakawa, Y.: Optimization of Current Distribution in an Applied-Field MPD Thruster. 20th International Electric Propulsion Conference Proceedings, AIAA, 1988, pp. 323-332.

19. Yoshikawa, T.; Kagaya, Y.; and Tahara, H.; Thrust Measurement of a Quasi-Steady MPD Arcjet. AIAA Paper 85-2003, Sept. 1985.

20. Cann, G.L.; Harder, R.L.; Moore, R.A.; and Lenn, P.D.: Hall Current Accelerator. (ESOC-5470-Final, Electro-Optical Systems Inc.; NASA Contract NAS3-5909) NASA CR-54705, 1966.

21. Bennett, S.; Enos, G.; John, R.; and Powers, W.: Magnetoplasmadynamic Thruster Research. (AVSSD-0272-67-RR, AVCO Corp.; NASA Contract NAS3-8907) NASA CR-72345, 1967.

22. Moore, R.A.; Cann, G.L.; and Gallagher, L.R.: High Specific Impulse Thermal ArcJet Thruster Technology. Part I. Performance of Hall Arc Jets With Lithium Propellant. Wright-Patterson AFB Technical Report, AFAPL-TR-65-48, Part I, June 1965. (Avail. NTIS, AD-465068).

23. Connolly, D.G.; Sovie, R.J.; and Seikel, G.R.: Performance and Diagnostics of a Water-Cooled Magnetoplasmadynamic Arc Thruster. NASA TN D-5836, 1970.

24. Saber, A.J.; and Jahn, R.G.: Anode Power Deposition in Quasi-Steady MPD Arcs. AIAA Paper 73-1091, Oct. 1973.

TABLE I. - THRUSTER CONFIGURATIONS

Thruster designations	Anode channel diameter, cm	Channel length,[a] cm	Anode flare half angle/length, cm
A	16.5	5.3	0/0
B	16.5	4.1	0/0
C	26	4.2	0/0
D	26	4.2	45°/1.1

[a]Upstream end of cathode to anode exit plane.
[b]Cathode diameter, 1.27 cm; cathode length, 2.2 cm.

TABLE II. - SYSTEM INTERLOCKS

Sensor	Action
Tank pressure > 0.08 Pa (6×10^{-4} torr)	1 or 2
Tank pressure > 130 Pa (1 torr)	1
Vacuum flange not in place	3
Power and instrument doors closed	3
Arc water flow < 0.06 liter/sec	3
Heater water flow < 0.06 liter/sec	3
Cathode water flow < 0.03 liter/sec (not used)	3
Arc current > 3000 A for > 0.5 sec	3 and 4
Hydrogen detector alarm	3
No nitrogen purge to roughing pumps	3
Low nitrogen pressure to pneumatic hydrogen valve	3
Anode water temperature high	3

Actions
1 Alarm on. Power, water flow propellant flow off.
2 Over-ride sensor with switch.
3 Power, water flow, propellant flow off.
4 Detector engaged after arc start.

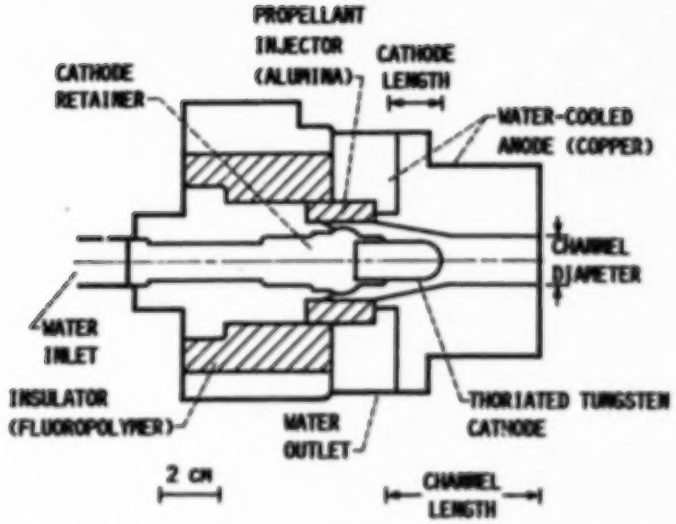

FIGURE 1. - MPD THRUSTER (A OR B) WITH CYLINDRICAL ANODE CHANNEL.

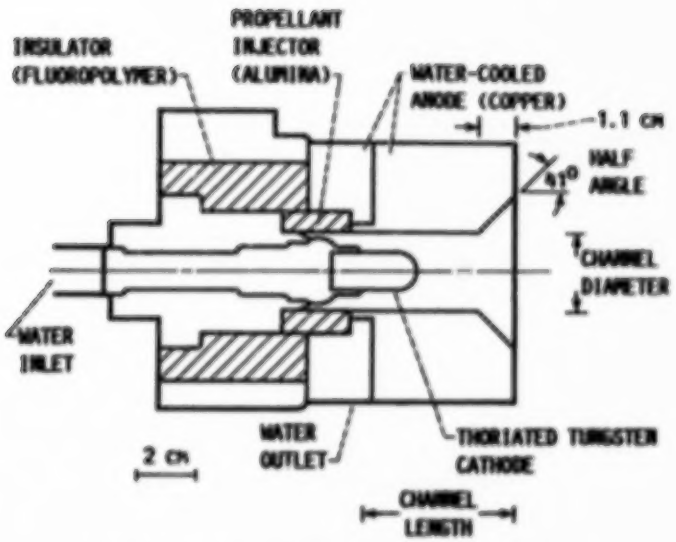

FIGURE 2. - MPD THRUSTER (D) WITH FLARED ANODE.

ORIGINAL PAGE IS
OF POOR QUALITY

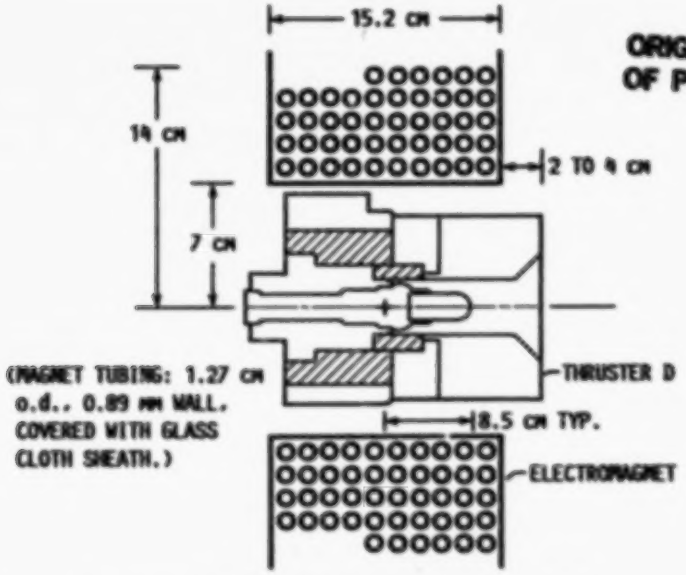

(A) SKETCH OF THRUSTER AND MAGNET ARRANGEMENT.

(B) PHOTOGRAPH OF THRUSTER AND ELECTROMAGNET INSTALLATION.

FIGURE 3. - MPD THRUSTER AND MAGNET ASSEMBLY.

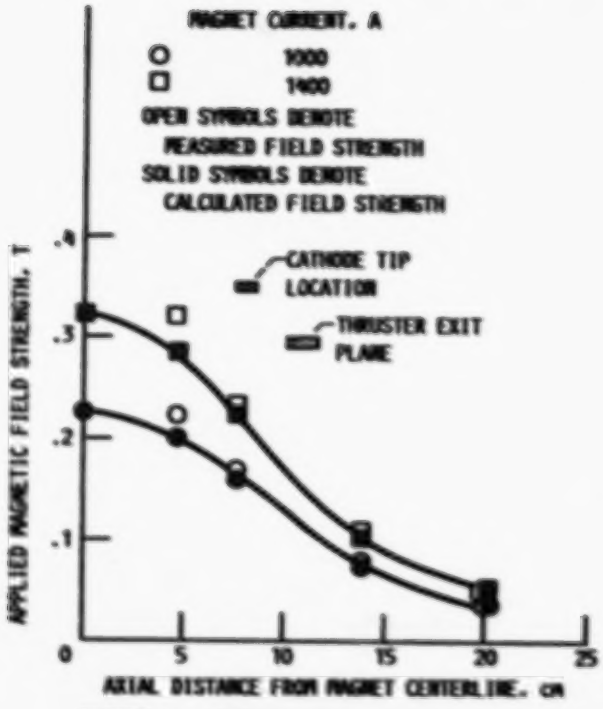

FIGURE 4. - COMPARISON OF CALCULATED AND MEASURED AXIAL MAGNETIC FIELD STRENGTH.

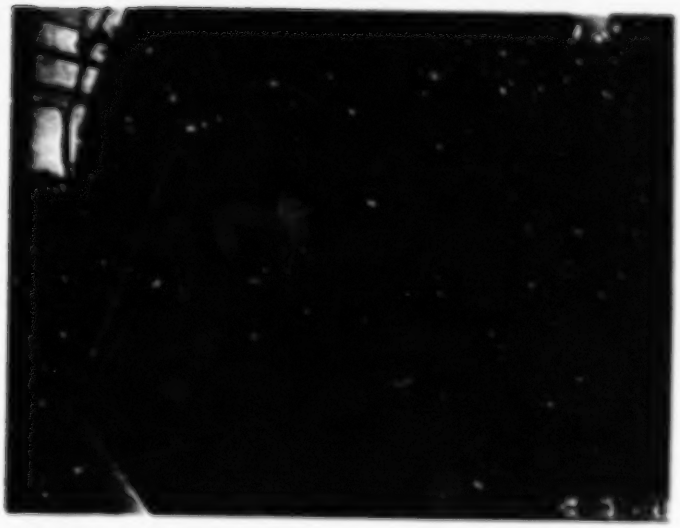

FIGURE 5. - THRUST STAND INSERTED INTO THE 3 m DIAMETER VACUUM SPOOL-PIECE.

ORIGINAL PAGE IS
OF POOR QUALITY

ORIGINAL PAGE IS
OF POOR QUALITY

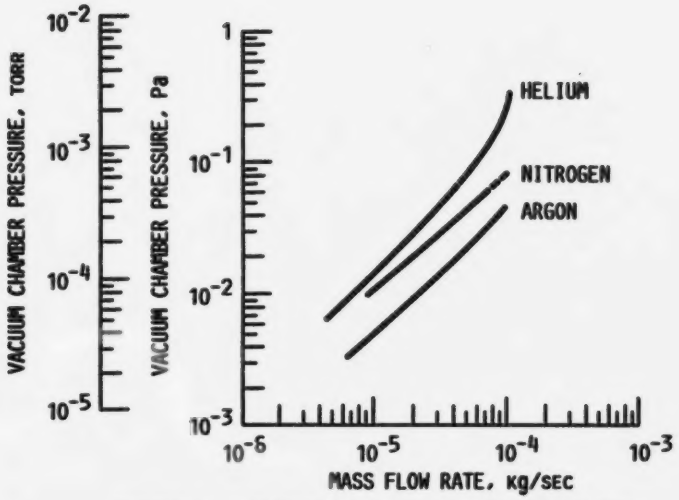

FIGURE 6. - VACUUM FACILITY PUMPING CAPABILITY WITH FIFTEEN OIL DIFFUSION PUMPS. PRESSURE MEASURED APPROXIMATELY 12 m FROM THRUSTER.

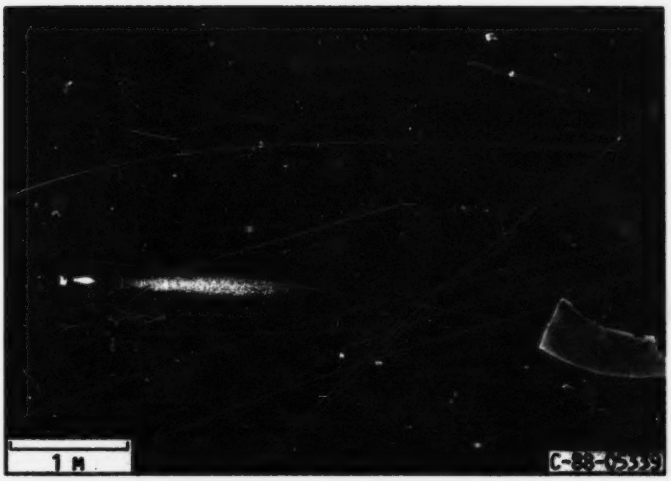

FIGURE 7. - PLUME FROM ARCJET OPERATING AT 130 kW WITH HELIUM PROPELLANT.

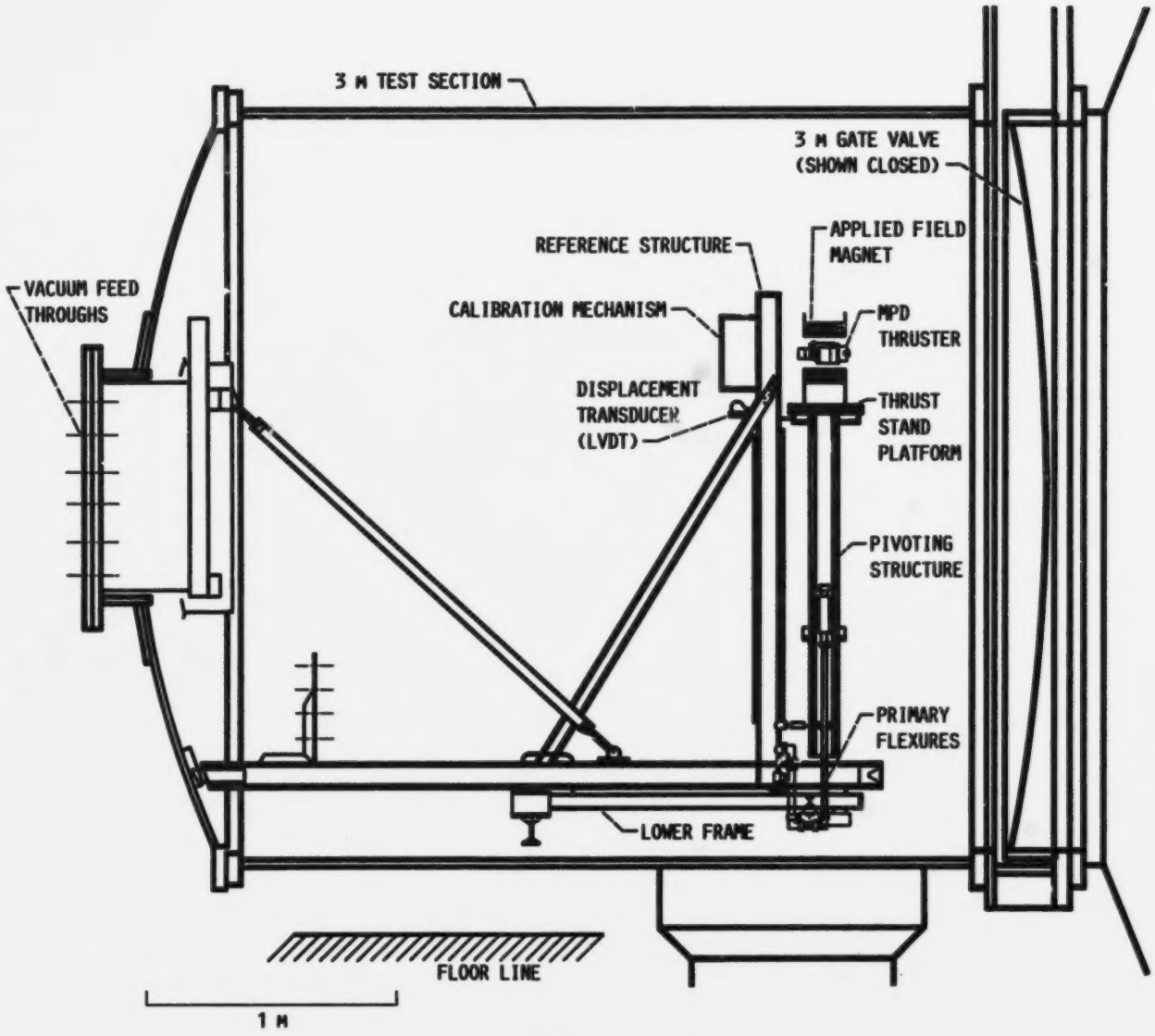

FIGURE 8. - SCHEMATIC OF THRUST STAND.

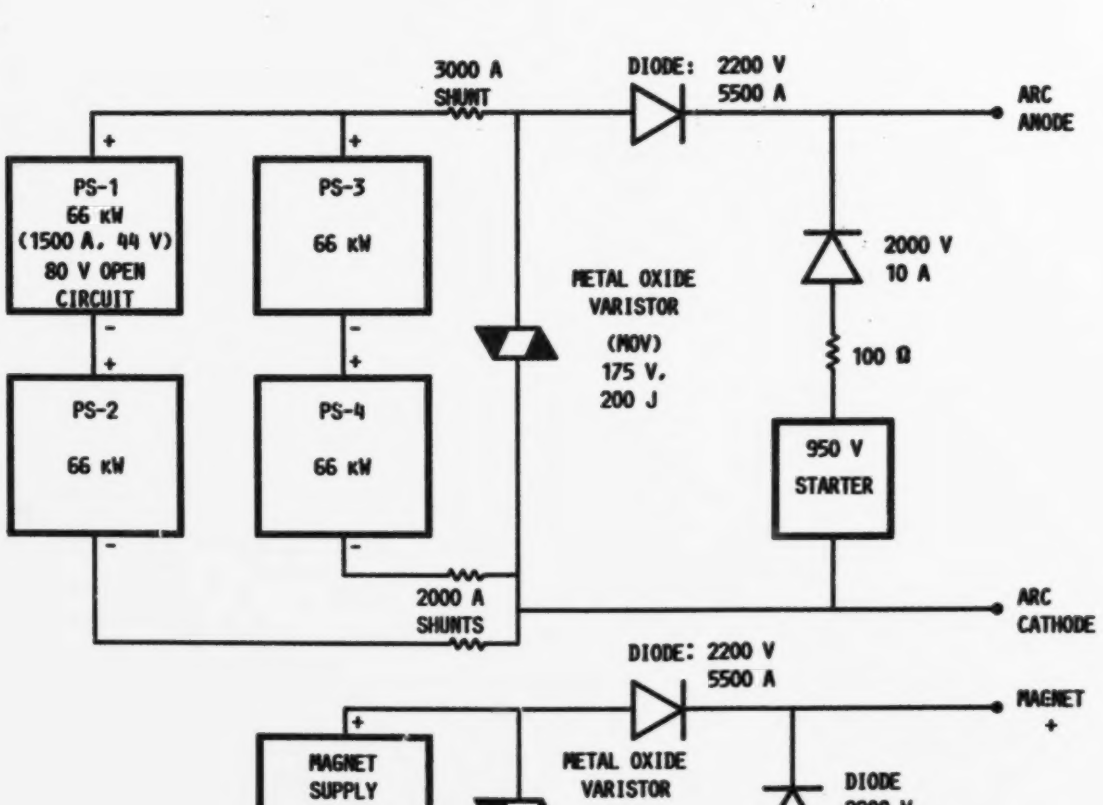

FIGURE 9. - POWER SYSTEM SCHEMATIC. (INPUT POWER: 30, 460 V; POWER CABLES: (FOUR EACH) 777 MCM CABLES FOR 3000 A.)

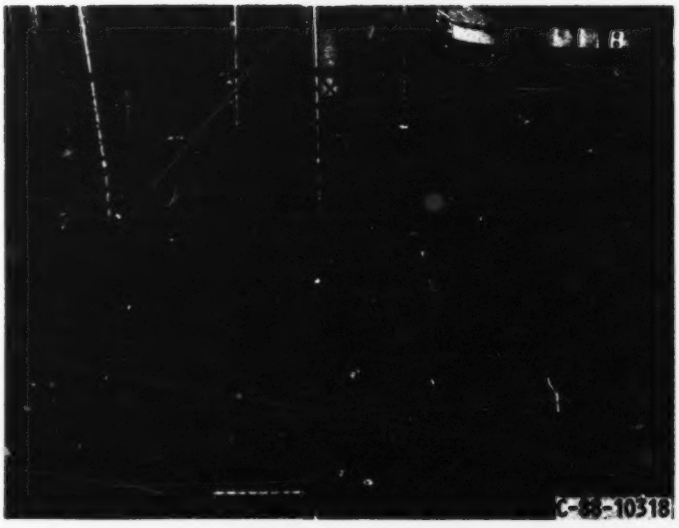

FIGURE 10. - PHOTOGRAPH OF FOUR ARC POWER SUPPLIES AND MAGNET SUPPLY.

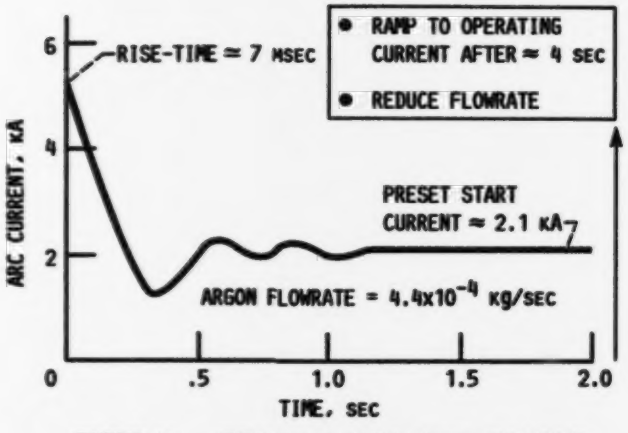

FIGURE 11. - TYPICAL ARC-START AFTER BREAKDOWN WITH IGNITOR SUPPLY.

ORIGINAL PAGE IS OF POOR QUALITY

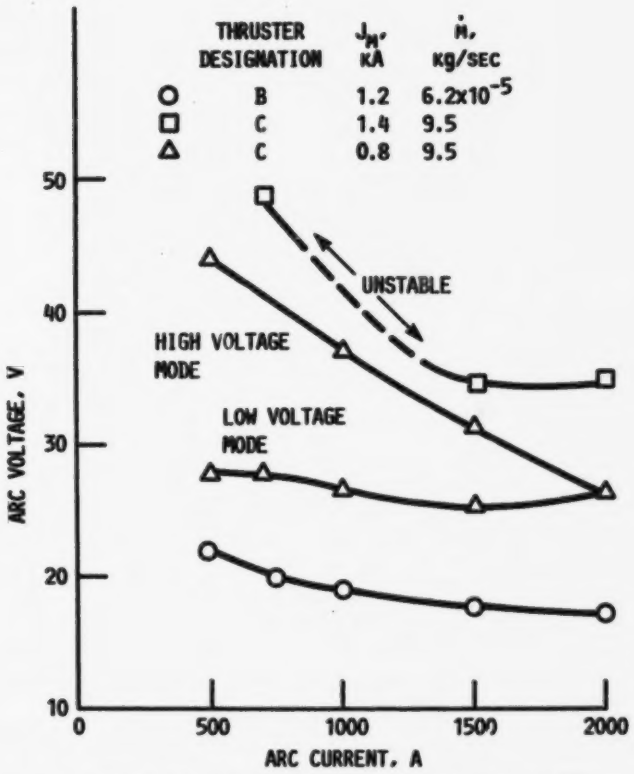

FIGURE 12. - MPD THRUSTER DISCHARGE CHARACTERISTICS WITH ARGON.

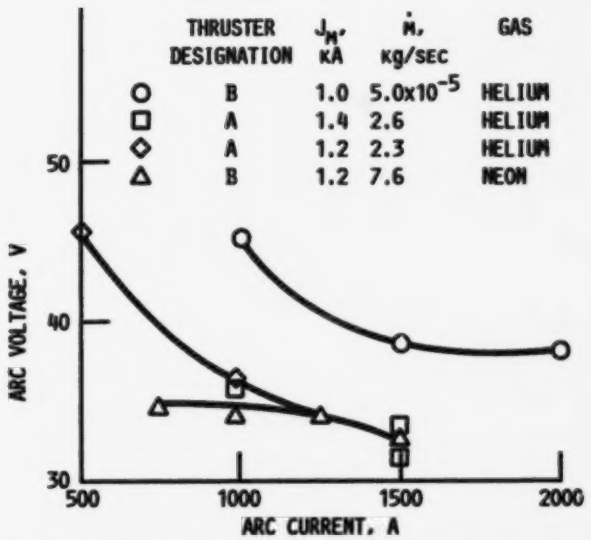

FIGURE 13. - MPD THRUSTER DISCHARGE CHARACTERISTICS WITH HELIUM AND NEON.

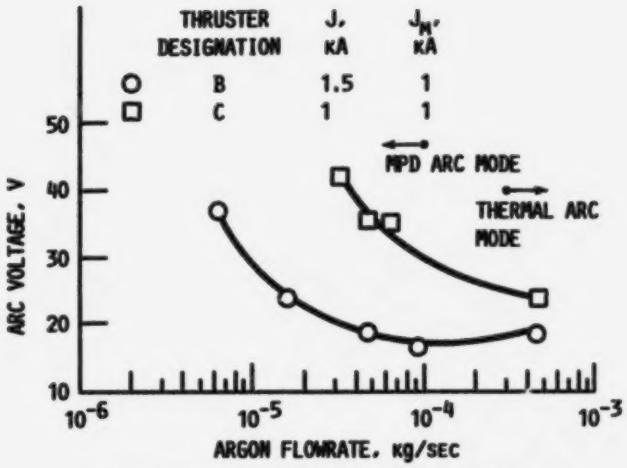

FIGURE 14. - SENSITIVITY OF ARC VOLTAGE TO ARGON MASS FLOWRATE.

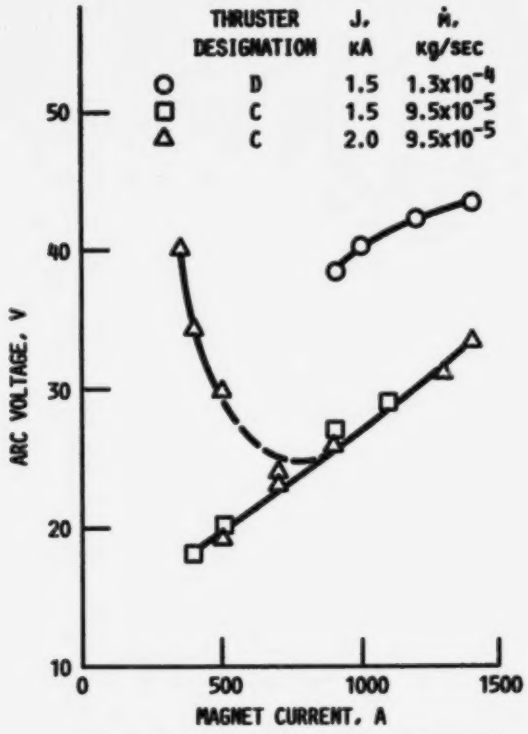

FIGURE 15. - EFFECT OF APPLIED MAGNETIC FIELD ON ARC VOLTAGE (ARGON PROPELLANT).

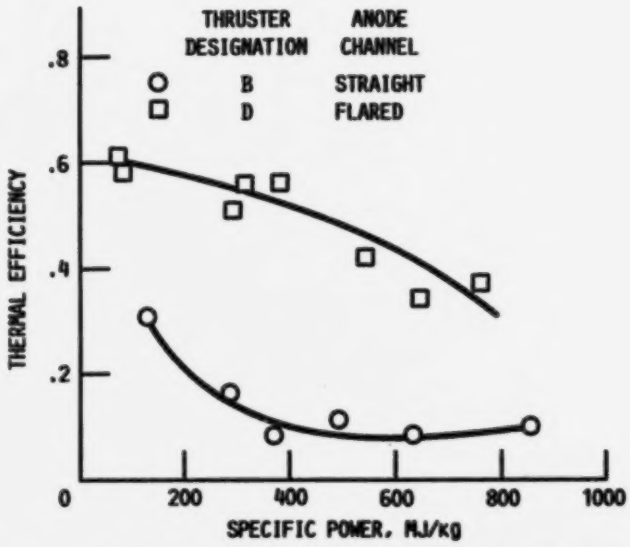

FIGURE 16. - EFFECT OF ANODE CONFIGURATION ON THERMAL EFFICIENCY (ARGON PROPELLANT).

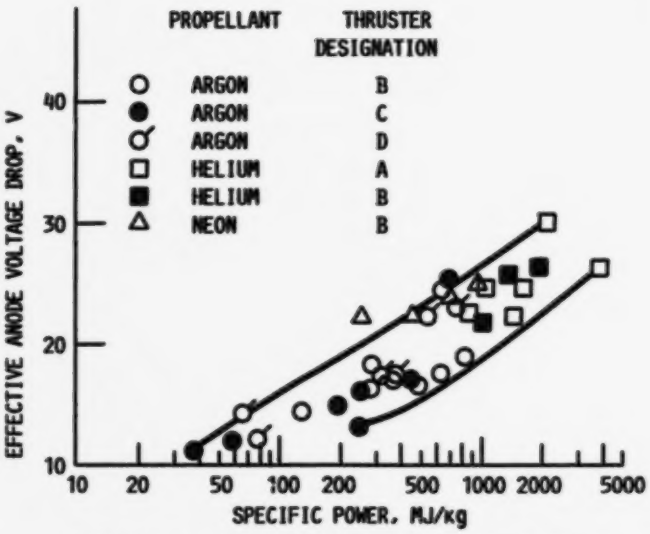

FIGURE 17. - EFFECTIVE ANODE FALL VOLTAGE VERSUS SPECIFIC POWER.

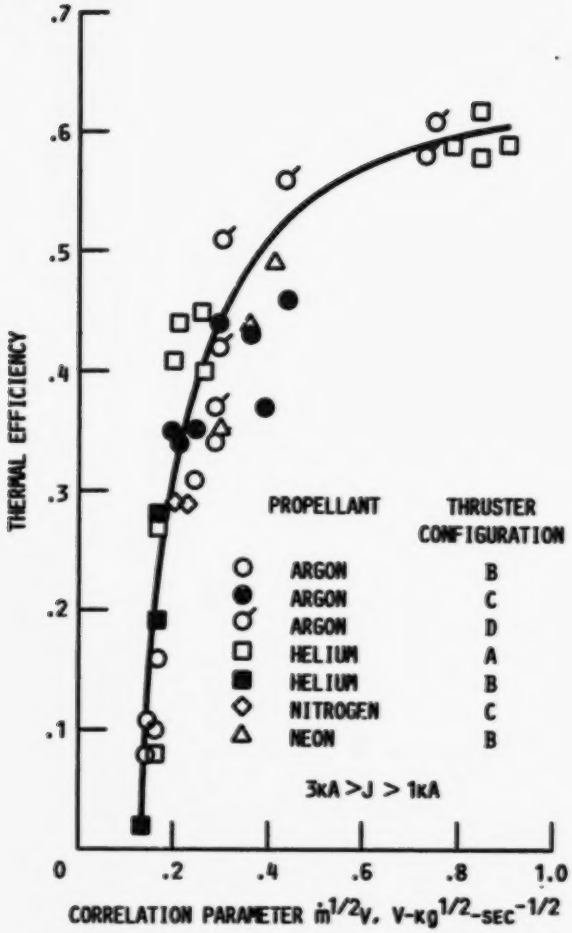

FIGURE 18. - THERMAL EFFICIENCY CORRELATION PARAMETER.

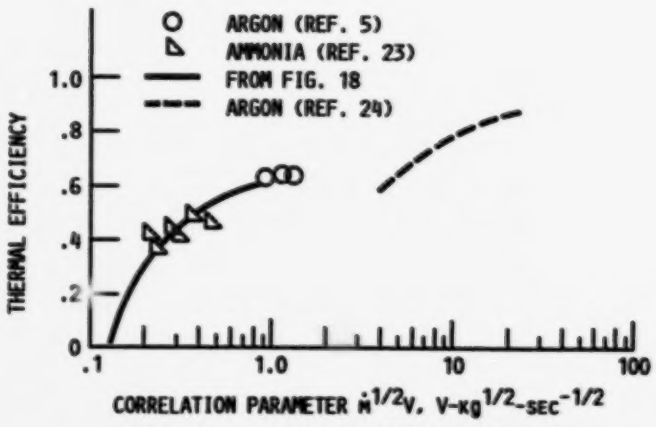

FIGURE 19. - THERMAL EFFICIENCY CORRELATIONS.

NASA
National Aeronautics and Space Administration

Report Documentation Page

1. Report No.	2. Government Accession No.	3. Recipient's Catalog No.
NASA TM-102021		

4. Title and Subtitle

Test Facility and Preliminary Performance of a 100 kW Class MPD Thruster

5. Report Date

6. Performing Organization Code

7. Author(s)

James S. Sovey, Maris A. Mantenieks, Thomas W. Haag, Paul Raitano, and James E. Parkes

8. Performing Organization Report No.

E-4742

10. Work Unit No.

506-42-31

9. Performing Organization Name and Address

National Aeronautics and Space Administration
Lewis Research Center
Cleveland, Ohio 44135-3191

11. Contract or Grant No.

13. Type of Report and Period Covered

Technical Memorandum

12. Sponsoring Agency Name and Address

National Aeronautics and Space Administration
Washington, D.C. 20546-0001

14. Sponsoring Agency Code

15. Supplementary Notes

Prepared for the 1989 JANNAF Propulsion Meeting, Cleveland, Ohio, May 23-25, 1989. James S. Sovey, Maris A. Mantenieks, Thomas W. Haag, and Paul Raitano, NASA Lewis Research Center. James E. Parkes, Sverdrup Technology, Inc., NASA Lewis Research Center Group, Cleveland, Ohio 44135.

16. Abstract

A 260 kW magnetoplasmadynamic thruster test facility was assembled and used to characterize thrusters at power levels up to 130 kW using argon and helium propellants. Sensitivities of discharge characteristics to arc current, mass flow rate, and applied magnetic field were investigated. A thermal efficiency correlation developed by others for low power MPD thrusters defined parametric guidelines to minimize electrode losses in MPD thrusters. Argon and helium results suggest that a parameter defined as the product of arc voltage and the square root of the mass flow rate must exceed 0.7 V-kg$^{(1/2)}$-s$^{(-1/2)}$ in order to obtain thermal efficiencies in excess of 60 percent.

17. Key Words (Suggested by Author(s))	18. Distribution Statement
Electric propulsion Plasmas MPD thruster	Unclassified – Unlimited Subject Category 20

19. Security Classif. (of this report)	20. Security Classif. (of this page)	21. No of pages	22. Price*
Unclassified	Unclassified	20	A03

NASA FORM 1626 OCT 86

*For sale by the National Technical Information Service, Springfield, Virginia 22161